Calculation of the third virial coefficient for water

P. G. Kusalik, F. Liden, and I. M. Svishchev
Department of Chemistry, Dalhousie University, Halifax, Nova Scotia, B3H 4J3, Canada

(Received 27 June 1995; accepted 7 September 1995)

Although the second virial coefficient has been used frequently to test intermolecular potentials, the direct calculation of third virial coefficients has only been attempted for atomic or simple (with linear symmetry) multipolar fluids. In this paper a general approach is described for the numerical evaluation of the third virial coefficient for molecular systems. Specific results for the second and third virial coefficients for several different water models are reported and compared with experimental data; critical points are also estimated. A polarizable model is found to be superior to standard effective liquid-phase potentials in reproducing the equation of state for steam. © *1995 American Institute of Physics.*

I. INTRODUCTION

The virial equation of state (VES) is a standard approach used to represent experimental data of real gases.[1,2] At sufficiently low density the relationship between the pressure p, density $\rho=N/V$, and temperature T of a fluid can be expressed as a power series in density

$$\frac{p}{\rho kT}=1+B\rho+C\rho^2+\ldots, \tag{1}$$

where k is the Boltzmann constant, and B and C are the second and third virial coefficients, respectively. By definition the first term in the virial expansion (1) represents ideal gas behavior with subsequent terms giving corrections for real systems. The special significance given to the VES arises primarily from the fact that the virial coefficients can be directly related to the interactions between the molecules of the system.[1,3] In particular, B depends upon interactions between pairs of molecules, while C involves the interaction energies of three molecule groupings. Thus the evaluation of virial coefficients, principally B, has served as a test for model interaction potentials.[1,4–10] Whereas the direct numerical integration (see below) of B has been performed for a variety of molecular models,[1] including water,[6–10] to our knowledge calculations of the third virial coefficient have been limited to molecules of linear symmetry.[5,11] Not only does C provide a more sensitive test of intermolecular potentials,[5] it also allows the prediction of critical points and phase instabilities. In this paper we describe a general numerical integration scheme for the determination of the third virial coefficient for molecules of arbitrary symmetry and report explicit results for several models for water, both polarizable and nonpolarizable. We find that effective condensed-phase potentials give rather poor results, while polarizable models achieve much better agreement with experimental data.

The remainder of this paper is organized as follows. In Sec. II we describe our methodology for the evaluation of the third virial coefficient, while in Sec. III we report results for three different water models. Our conclusions are summarized in Sec. IV.

II. METHOD OF INTEGRATION

It can be shown[1,2] that the second virial coefficient appearing in Eq. (1) can be represented as

$$B=-\frac{1}{2}\left\langle \int f_{12}\, d\mathbf{r}_{12}\right\rangle_{\Omega_1\Omega_2}, \tag{2}$$

in which $\langle\cdots\rangle$ denotes the appropriate average over molecular orientations, Ω_1 and Ω_2, and

$$f_{\alpha\beta}=\exp[-u_{\alpha\beta}/kT]-1 \tag{3}$$

is a Mayer-f function, where $u_{\alpha\beta}$ is the total pair interaction energy between particles α and β. For systems in which the energy may not be pairwise additive, we can write the third virial coefficient as[1]

$$C(T)=C_{\text{add}}+\Delta C, \tag{4a}$$

for which

$$C_{\text{add}}=\frac{-1}{3}\left\langle \int\int f(12)f(13)f(23)d\mathbf{r}_{12}\, d\mathbf{r}_{13}\right\rangle_{\Omega_1\Omega_2\Omega_3} \tag{4b}$$

is the contribution due to pairwise additive terms in the potential, and

$$\Delta C=\frac{-1}{3}\left\langle \int\int [e^{-\Delta u_{123}/kT}-1] \times e^{-(u_{12}+u_{13}+u_{23})/kT}\, d\mathbf{r}_{12}\, d\mathbf{r}_{13}\right\rangle_{\Omega_1\Omega_2\Omega_3} \tag{4c}$$

arises due to three-body terms. In Eqs. (4)

$$\Delta u_{123}=u_{123}-(u_{12}+u_{13}+u_{23}), \tag{5}$$

where u_{123} is the full three-body energy, and

$$\langle\cdots\rangle_{\Omega_1\Omega_2\Omega_3}=\frac{1}{(8\pi^2)^2}\int_0^{2\pi}d\phi_2\int_0^{2\pi}d\chi_2\int_0^{\pi}\sin\theta_2\, d\theta_2 \times\int_0^{2\pi}d\phi_3\int_0^{2\pi}d\chi_3\int_0^{\pi}\sin\theta_3\, d\theta_3, \tag{6}$$

in which $\Omega_\alpha=(\phi_\alpha,\chi_\alpha,\theta_\alpha)$ and we have chosen (without loss of generality) our reference frame to be fixed on particle 1. For water, Eq. (6) simplifies by symmetry to

$$\langle\cdots\rangle_{\Omega_1\Omega_2\Omega_3}=\frac{1}{(2\pi^2)^2}\int_0^{\pi}d\phi_2\int_0^{\pi}d\chi_2\int_0^{\pi}\times\sin\theta_2\,d\theta_2\int_0^{\pi}d\phi_3\int_0^{\pi}d\chi_3\int_0^{\pi}\sin\theta_3\,d\theta_3. \tag{7}$$

For a molecular system such as water, B requires the evaluation of a 6-dimensional integral. This numerical task can now be performed almost routinely using nonproduct integration methods.[6–10] However, the determination of C involves an imposing 12-dimensional numerical integration; consequently, we are aware of no previously published calculations of C for systems without at least linear symmetry. Recently, Joslin and Goldman[11] reported results for the third virial coefficient of a dipolar hard-sphere fluid (where C can be expressed as a 9-dimensional integral). The integration methods we have employed exploit some of the techniques used by these workers but there are also several important differences. As the successful evaluation of Eqs. (4) depends critically upon the particular methods used, we describe below the key steps in our approach.

A. Partitioning of the integration region

Similar to Joslin and Goldman,[11] we rewrite the volume integrals in Eqs. (4) in the form

$$I\equiv\int\int d\mathbf{r}_{12}\,d\mathbf{r}_{13}=\int_0^{2\pi}d\phi_{12}\int_0^{\pi}\sin\theta_{12}\,d\theta_{12}\int_0^{2\pi}d\phi_{23}\times\int_0^{\pi}\sin\theta_{23}\,d\theta_{23}\int_0^{\infty}\int_0^{\infty}r_{12}^2r_{13}^2\,dr_{12}\,dr_{13}, \tag{8}$$

where we have chosen to define $\mathbf{r}_{13}$ relative to $\mathbf{r}_{12}$ through the angles θ_{23} and ϕ_{23}. From simple trigonometry we have

$$I=\int_0^{2\pi}d\phi_{12}\int_0^{\pi}\sin\theta_{12}\,d\theta_{12}\int_0^{2\pi}d\phi_{23}\times\int_0^{\infty}r_{12}\,dr_{12}\int_0^{\infty}r_{13}\,dr_{13}\int_{|r_{12}-r_{13}|}^{r_{12}+r_{13}}r_{23}\,dr_{23}, \tag{9}$$

where the limits on the final integral follow from the triangular inequality

$$|r_{12}-r_{13}|\leqslant r_{23}\leqslant r_{12}+r_{13}. \tag{10}$$

Like Joslin and Goldman[11] we also divide our integral into four parts, region 1 with no ''overlaps,'' region 2 with one overlap, region 3 with two overlaps, and region 4 with all three particles overlapping. We consider two particles α and β to overlap when

$$r_{\alpha\beta}<r_{sw}, \tag{11}$$

in which r_{sw} is an adjustable parameter.

In addition to these steps, we take advantage of the fact that only unique triple arrangements need be considered. Thus in evaluating C, we always require

$$r_{12}\geqslant r_{13}\geqslant r_{23} \tag{12}$$

and then multiply the numerical result by $6=3!$, the number of permutations of the arrangement. Subject to the restriction in Eq. (12) the triangular inequality (10) becomes

$$r_{12}-r_{13}\leqslant r_{23}\leqslant r_{12}+r_{13}. \tag{13}$$

It is easy to show that conditions (12) and (13) can only hold simultaneously if

$$r_{13}\geqslant r_{12}/2. \tag{14}$$

For water the integration in Eq. (9) can therefore be expressed as

$$I=12\int_0^{\pi}d\phi_{12}\int_0^{\pi}\sin\theta_{12}\,d\theta_{12}\int_0^{2\pi}d\phi_{23}\times\int_0^{\infty}r_{12}\,dr_{12}\int_{r_{12}/2}^{r_{12}}r_{13}\,dr_{13}\int_{r_{12}-r_{13}}^{r_{13}}r_{23}\,dr_{23}. \tag{15}$$

Given the restrictions imposed by conditions (11)–(14), we can specifically define the limits for each of our integration regions. For region 1

$$r_{12}\geqslant r_{13}\geqslant r_{23}\geqslant r_{sw} \tag{16a}$$

and the limits of integration become

$$r_{\max}\geqslant r_{12}\geqslant r_{sw}, \tag{16b}$$

$$r_{12}\geqslant r_{13}\geqslant \mathrm{Max}[r_{sw},r_{12}/2], \tag{16c}$$

$$r_{13}\geqslant r_{23}\geqslant \mathrm{Max}[r_{sw},r_{12}-r_{13}]; \tag{16d}$$

for region 2

$$r_{12}\geqslant r_{13}\geqslant r_{sw}\geqslant r_{23} \tag{17a}$$

and

$$r_{\max}\geqslant r_{12}\geqslant r_{sw}, \tag{17b}$$

$$r_{12}\geqslant r_{13}\geqslant \mathrm{Max}[r_{sw},r_{12}-r_{sw}], \tag{17c}$$

$$r_{sw}\geqslant r_{23}\geqslant r_{12}-r_{13}; \tag{17d}$$

for region 3

$$r_{12}\geqslant r_{sw}\geqslant r_{13}\geqslant r_{23} \tag{18a}$$

and

$$2r_{sw}\geqslant r_{12}\geqslant r_{sw}, \tag{18b}$$

$$r_{sw}\geqslant r_{13}\geqslant r_{12}/2, \tag{18c}$$

$$r_{13}\geqslant r_{23}\geqslant r_{12}-r_{13}; \tag{18d}$$

for region 4

$$r_{sw}\geqslant r_{12}\geqslant r_{13}\geqslant r_{23} \tag{19a}$$

and

$$r_{sw}\geqslant r_{12}\geqslant 0, \tag{19b}$$

$$r_{12}\geqslant r_{13}\geqslant r_{12}/2, \tag{19c}$$

$$r_{13}\geqslant r_{23}\geqslant r_{12}-r_{13}. \tag{19d}$$

In each case, these limits were confirmed by recovering the values of the appropriate volume integrals.

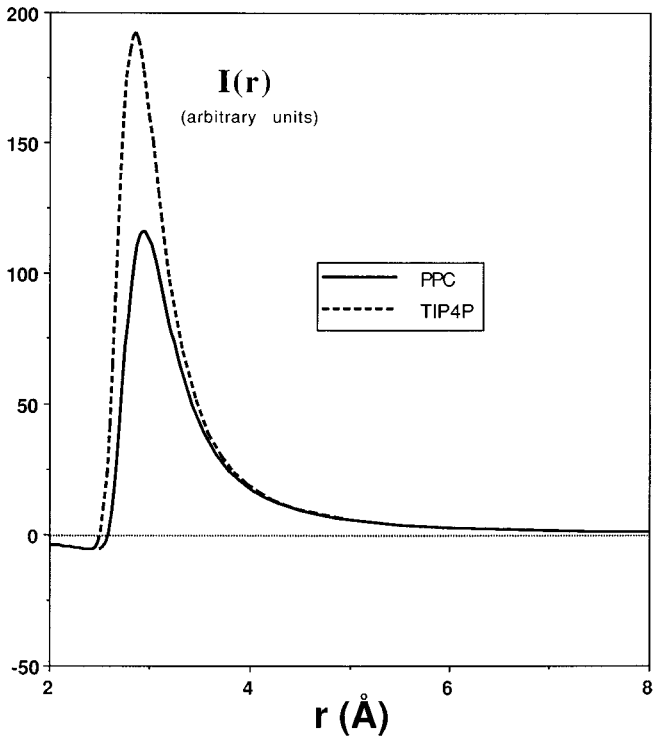

FIG. 1. Second virial integrand upon integration over all angular variables. Results for two water models at a temperature of 423 K are shown.

A separation of 2.6 Å was found to be a good choice for r_{sw} (although the quality of the results did not appear strongly sensitive to its exact value) and this value was used for each of the water models investigated here. We remark that this separation is only somewhat larger than the hard cores which, for computational convenience, were inserted into each of the models. An integration upper bound of $r_{\max}=10$ Å proved to be sufficient and was employed throughout.

B. Choice of integration variables

We have found that a strategic choice of integration variables is necessary to facilitate the evaluation of the third virial coefficient. To demonstrate the sensitivity of virial coefficient integrands to particle separations, we have shown in Fig. 1 the result of integrating over all five angular variables in Eq. (2). The ''areas'' under the curves plotted in Fig. 1 would give values for B (to within a constant factor). We see that for both potentials the value of this integrand varies rather dramatically for separations near contact (i.e., 2.5–4.0 Å) and that this same region must dominate the final value of B. Clearly, nonuniform sampling of separations is desirable. Following previous workers[11] we considered the transformation

$$x_{\alpha\beta}=1/r_{\alpha\beta}. \tag{20a}$$

Further, the transformations

$$x_{\alpha\beta}=1/r_{\alpha\beta}^2 \tag{20b}$$

and

$$x_{\alpha\beta}=1/\sqrt{r_{\alpha\beta}} \tag{20c}$$

were also explored. Through extensive testing, we found that Eq. (20a) gave generally superior results when the transformation of separation variables was beneficial. In our calculations for water, both r_{12} and r_{13} were transformed for region 1, while for region 2 Eq. (20a) was applied to r_{12} only and no transformation was employed for regions 3 and 4.

Transformation of some of the angular variables also proved to be advantageous. In particular,

$$x_{\alpha\beta}=\tfrac{1}{2}(\cos\,\theta_{\alpha\beta}+1) \tag{21}$$

was exploited throughout our calculations.

C. Integration algorithm

The high dimensionality, 6 and 12, respectively, of the integrals involved in the evaluation of B and C necessitates the use of nonproduct methods. In our calculations of the second virial coefficients, we successfully implemented the quasi-Monte Carlo approach of Conroy.[12] However, in our work with third virial coefficients we have exploited library routines, in particular those available through NAG.[13] Four alternatives provided by Mk. 15 of the NAG Library were considered: (1) the number-theoretical method of Korobov–Conroy[12,14] as implemented in the routine D01GCF, (2) the adaptive Monte Carlo method of Lautrup[15] as implemented in D01GBF, (3) the method of Sag and Szeheres[16] in the D01FDF, and (4) the routine D01FCF which uses an adaptive subdivision strategy.[17] After extensive comparison with both test and Mayer-f functions [Eq. (3)] in 6, 9, and 12 dimensions we found that D01GCF consistently outperformed the other methods. We remark that Joslin and Goldman[11] chose the routine D01GBF in their work, claiming it gave superior results. We did observe that the quality of the results produced by the routine D01GCF were rather sensitive to the specific number sets used, and hence considerable effort was expended in determining optimal choices of number sets. Details of our choice of number sets can be found in Appendix A. In our testing we also observed essentially a $1/N$ dependence, where N is the number of integration points, on the average error in the estimates produced by D01GCF; for D01GBF this apparent dependence was only $1/\sqrt{N}$.

In order to obtain estimates for the standard error, the routine D01GCF incorporates a stochastic integration rule through the inclusion of a random origin shift. Thus a given numerical integration can be repeated n_r times from which an error estimate can be computed. Like Joslin and Goldman,[11] we did find that the errors provided by D01GCF were not always reliable, particularly for smaller n_r (i.e., $\leqslant 5$). Yet, to take full advantage of this number-theoretical method, we attempted to keep n_r small (since the estimate for the integral will converge only as $1/\sqrt{n_r}$) while maintaining N large. All the results presented in this paper were obtained using a total of 30 million function evaluations[18] (16 million for region 1, 8 million for region 2, 4 million for region 3, and 2 million for region 4) with $n_r=2$. Supplementary calculations were performed for each model at several different temperatures using an entirely different number set

TABLE I. Contributions to the third virial coefficient from the four integration regions. The results given are for TIP4P water with $r_{sw}=2.6$ Å and are in units of cm^6/mol^2.

T (K)	C_1	C_2	C_3	C_4	C
423	−297 600	171 100	−2260	141	−128 600
523	−17 380	32 140	−2220	207	12 750
623	−315	10 280	−1445	236	8 760
723	1190	4370	−980	250	4830

with $n_r=7$ for a total of 50 million function evaluations. This second set of integrations served not only to check the reliability of our data, they also provided more direct information on our errors. In addition, several integrations involving 100–150 million function evaluations were carried out for select points to provide further confirmation of our values and error estimates. A typical integration using 30–50 million points required between 10–20 h on a single i860 processor on an Alliant FX2800 for the nonpolarizable models studied. For our polarizable model the time required roughly doubled.

As a test of our integration methodology we reproduced some of the third virial coefficient data reported previously[11] for dipolar hard spheres. These calculations were carried out both as 12 and as 9 dimensional integrations, the former strictly for testing purposes. For a reduced dipole moment of 2.0 we were able to evaluate the integral for region 1 with less than 1% error with fewer than 40 million function evaluations. This appears to improve considerably upon the computational effort required by the approach of previous workers[11] utilizing the NAG routine D01GBF (for which several hundred million points were apparently used). One easily identified advantage of the routine D01GCF over D01GBF is a greater flexibility in specifying the limits of integration in the former allowing a greater reduction of the integral [as discussed above in Eqs. (12)–(19)].

D. Second virial coefficient

The values of the second virial coefficient report in this study were determined by first integrating over all five angular variables in Eq. (2) using the method of Conroy[12] (see Fig. 1) followed by Simpson's rule integrations on multiple separation grids. This approach, which required a total of 400 000 points to achieve an error of about 1%, was again tested by reproducing previously published data.[8,9] Adapting many of the methods described above for the third virial coefficient to the calculation of B, we can obtain values to within about 1% error with as few as 150 000 function evaluations. We remark that previous workers[7–10] using various other methods have typically used several hundred thousand points in their integrations.

III. RESULTS AND DISCUSSION

Three different models for water were considered in this study. The SPC/E[19] and TIP4P[20] models are based on effective condensed-phase potentials that have been shown to reproduce successfully many of the properties of liquid water under ambient conditions.[20] The polarizable point-charge (PPC) potential[21] is a simple three charge-site model which explicitly incorporates molecular polarizability (see Appendix B). It has been found that the PPC model[21,22] successfully reproduces many of the properties of liquid water, including the dielectric constant, over the temperature range −10 to 300 °C.

Table I contains representative values of the contributions to the third virial coefficient from each of the four integration regions. The error for any specific integration is typically less than 5%, and we estimate our uncertainty in C to be less than 10% in almost all cases. The contribution to the third virial coefficient from region 1 (with no overlaps) proved to be the most difficult to evaluate, particularly at lower temperatures. We can see from Table I that this contribution dominates the value of C at lower temperatures, but decreases in magnitude and eventually changes sign as T is increased. Full tables of the calculated second and third virial coefficients for TIP4P, SPC/E, and PPC water can be found in Appendix C.

Figure 2 compares results for the second virial coefficient for the three models with data from experiment. Both effective potentials, SPC/E and TIP4P, poorly reproduce the

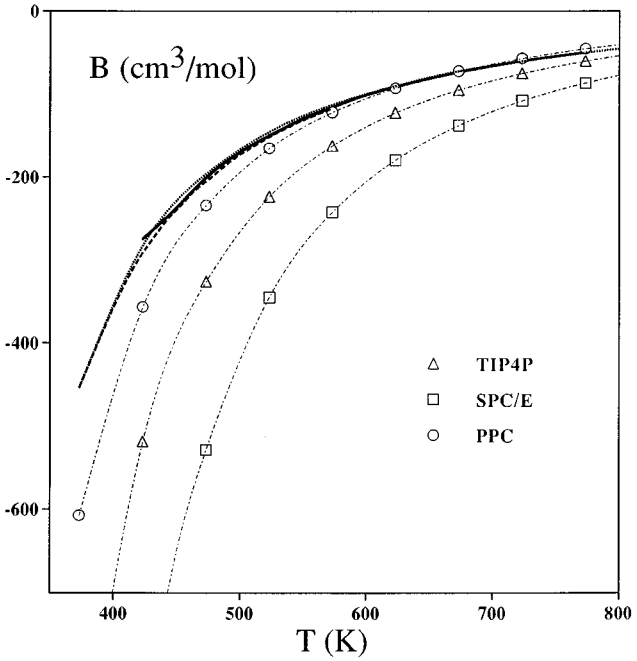

FIG. 2. The second virial coefficient. Results for the SPC/E, TIP4P, and PPC models are shown along with the experimental data of Hill and MacMillan (Ref. 23) (dashed line), Kell, McLaurin, and Whalley (Ref. 24) (solid line), and Vulalovich, Trakhtengerts, and Spiridonov (Ref. 25) (dotted line).

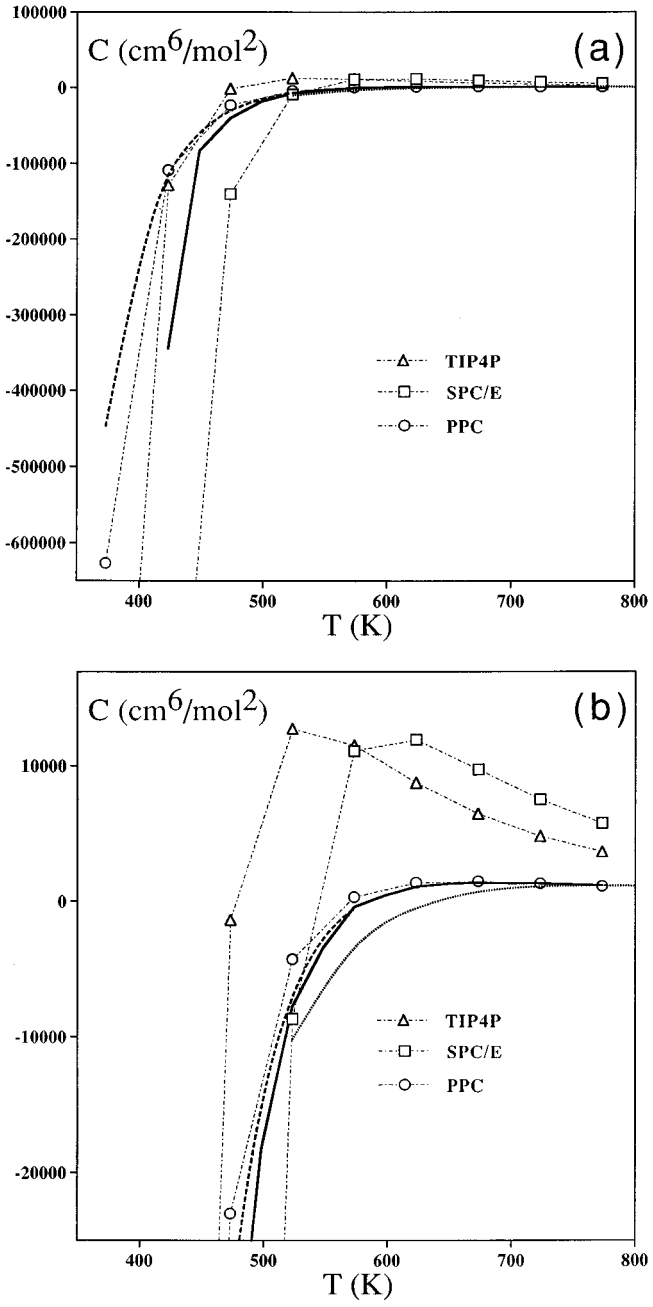

FIG. 3. The third virial coefficient. Results for the SPC/E, TIP4P, and PPC models are shown along with the experimental data of Hill and MacMillan (Ref. 23) (dashed line), Kell, McLaurin and Whalley (Ref. 24) (solid line), and Vulalovich, Trakhtengerts, and Spiridonov (Ref. 25) (dotted line). (b) shows a greatly expanded view of (a).

experimental second virial coefficient, particularly at lower temperatures where the differences exceed 100%. As can be clearly seen from Fig. 2, the PPC model follows the experimental curves more closely than either of the two nonpolarizable models over the entire temperature range. Previous workers[9] have similarly noted the superiority of polarizable models in reproducing second virial coefficients for water.

A comparison of the third virial coefficients for the SPC/E, TIP4P, and PPC potentials with those of real water (see Fig. 3) reveals even more dramatically the behavior observed for B. We find that the two effective potentials are

TABLE II. Critical constants for water and for various water models.

Model (method)	T_c (K)	ρ_c (g/cm^3)	p_c (bar)
SPC/E (MD)[b]	652	0.326	189
SPC/E (virial)	613	0.095	88
TIP4P (virial)	549	0.096	80
PPC (virial)	698	0.281	298
Experiment (virial)[a]	712	0.286	310
Experiment (measured)	647	0.32	221

[a]Using data from Ref. 24 in the virial equation of state as discussed in the text.
[b]Reference 29.

only able to reproduce qualitatively the dependence of C upon temperature. We can see from Fig. 3 that unlike the second virial coefficient, there appears to be considerable variability in the estimates for C obtained from experiment. Our results for the PPC model are essentially in agreement with the available experimental data to within this apparent uncertainty.

When expanded beyond second order, the virial equation of state can be used to estimate the liquid–gas critical point.[1,11] Truncated at third order, the VES predicts that

$$B_c^2 = 3C_c, \tag{22a}$$

$$\rho_c = 1/B_c, \tag{22b}$$

and

$$\frac{p_c}{\rho_c k T_c} = \frac{1}{3}, \tag{22c}$$

where the subscript c denotes values at the critical point. Estimates for the critical points for the SPC/E, TIP4P, and PPC models for water were determined from Eqs. (22). These results are compared with experimental values in Table II.

Near the critical point the VES is no longer convergent and hence the usefulness of Eqs. (22) might be questioned. To provide some measure of the reliability of the values provided by these expressions, *experimental* data for the second and third virial coefficients for Ar,[26] N_2,[27] CH_4,[28] and water[24] were used in Eqs. (22) to estimate the critical points for these fluids. The results for water have been included in Table II where we see that the predicted critical temperature and density agree surprisingly well (to within 10% and 12.5% error, respectively) with the measured values. The critical pressure is not as successfully reproduced, but it is known that the value of the compressibility factor for water at its critical point deviates substantially from 1/3.[2] For Ar, N_2, and CH_4 the agreement between the estimated and measured values of the critical constants, including the pressure, is good with typical errors of less than 10% (which is comparable to the error in the original experimental virial data).

From Table II we see that while the critical point estimated by the VES for the PPC potential is close to that of real water, the critical constants predicted for the two effective models, particularly ρ_c, differ substantially from the measured values. However, a recent computer simulation study[29] reports a critical point for SPC/E water (see Table II)

TABLE III. Optimal coefficient sets used in numerical integrations.

	N							
	1 029 493	1 099 901	1 899 829	2 048 129	3 871 463	409 963	7 881 793	15 820 279
a_1	1	1	1	1	1	1	1	1
a_2	146 382	409 311	1 109 248	202	1 411 637	2 509 122	4 674 836	5 888 200
a_3	852 115	774 203	1 174 167	40 804	3 455 872	574 221	7 722 006	14 258 387
a_4	926 050	626 726	1 326 663	49 892	2 384 701	3 926 429	3 148 057	7 035 554
a_5	619 311	335 160	235 169	1 885 668	2 171 925	535 142	2 757 842	3 777 585
a_6	888 208	622 436	922 409	2 001 071	3 283 005	822 418	5 327 194	6 105 511
a_7	933 500	932 867	832 876	734 929	2 987 238	1 932 777	3 746 976	9 082 509
a_8	932 124	992 586	92 667	990 370	140 243	892 595	1 532 736	14 809 087
a_9	261 627	436 371	436 371	1 386 227	555 478	1 336 290	6 587 547	3 649 761
a_{10}	343 914	726 793	1 426 730	1 472 310	3 310 003	2 726 613	7 548 450	2 602 136
a_{11}	611 448	745 559	1 845 460	427 915	3 681 192	1 945 451	1 200 868	4 444 537
a_{12}	859 716	167 201	1 367 093	417 412	776 387	667 156	6 602 640	5 914 346

that is much closer to the experimental point; this is an unexpected finding in light of the present data and the behavior demonstrated in Figs. 2 and 3.

IV. CONCLUSIONS

In this paper we have reported the first third virial coefficients directly determined for a system of nonlinear molecules. We have presented a general scheme for performing these formidable numerical integrations. For a system such as water we were able to determine values for the third virial coefficient to within 10% uncertainty with only 30 million function evaluations. Results for three different water models, the TIP4P, SPC/E, and PPC potentials, were obtained and have been compared with recent experimental data. The effective liquid-phase potentials, SPC/E and TIP4P, were found to be in much poorer agreement with experimentally determined second and third virial coefficients than an explicitly polarizable potential, the PPC model. A critical point for each of the model systems has been estimated from our values of B and C; the PPC result was found to be superior, particularly for the critical density, to those predicted for either SPC/E or TIP4P water. The application of the numerical approach used in this study to other simple molecular systems, both single component and mixtures, and to the calculation of other virial (e.g., dielectric) coefficients should be straightforward.

ACKNOWLEDGMENTS

We are grateful for the financial support of the Natural Sciences and Engineering Research Council of Canada.

APPENDIX A: CHOICE OF OPTIMAL COEFFICIENT SETS

The quality of the approximation to a multidimensional integral provided by the Korobov–Conroy number-theoretical method[13,14] is sensitive to the particular set of coefficients, $\{a_1,a_2,\ldots,a_{12}\}$, used in the numerical calculation. The NAG library routine D01GZF was employed to determine sets of ''optimal'' coefficients. This routine requires that the total number of points, N, be the product of two prime numbers. The use of D01GZF (rather than D01GYF) was necessitated by the rather large values of N desired. Table III summarizes the values of N and their appropriate coefficients sets used in the present calculations.

APPENDIX B: THE POLARIZABLE POINT-CHARGE (PPC) MODEL

The polarization response of a water molecule, as measured by the dependence of its molecular dipole moment and values of its atomic site charges, was determined from high-level quantum chemical calculations. This response was then parameterized in terms of three site charges and the position of the negative site. The values of the hydrogen charges are given by (as obtained from Natural Population Analysis)

$$q_+ = 0.486 \pm 0.03E_x + 0.02E_z, \tag{B1}$$

where the sign of the X term changes with hydrogen 1 or 2, the electric field is given in V/Å, and the Z direction is defined to be along the axis of symmetry and the molecule lies in the XZ plane. The charge on the negative site follows from charge neutrality. The hydrogen sites are fixed at their optimized zero-field positions (with an OH bond length of 0.943 Å and a bond angle of 106°). The position (in Å) of the negative charge was parameterized to fit the local field dependence of the total dipole moment of the molecule and is given by

$$l_z = 0.11 - 0.03E_z \tag{B2a}$$

and

$$l_x = -0.025E_x. \tag{B2b}$$

To preserve the planar geometry of this simple 3-site model, no Y polarization was considered. The components of the polarizability for the PPC model,

$$\alpha_{xx} = 1.01 \ \text{Å}^3, \tag{B3a}$$

$$\alpha_{yy} = 0 \ \text{Å}^3, \tag{B3b}$$

and

$$\alpha_{zz} = 0.66 \ \text{Å}^3, \tag{B3c}$$

TABLE IV. Detailed numerical data for the second and third virial coefficients for the TIP4P, SPC/E, and PPC models.

	TIP4P		SPC/E		PPC	
Temp. (K)	B (cm^3/mol)	C (cm^6/mol^2)	B (cm^3/mol)	C (cm^6/mol^2)	B (cm^3/mol)	C (cm^6/mol^2)
373	−946	−1 290 000	−1856	−10 700 000	−607	−627 000
423	−519	−128 600	−907	−1 080 000	−357	−109 000
473	−326	−1 375	−529	−140 000	−234	−23 000
523	−224	12 750	−345	−8 660	−165	−4 290
573	−162	11 500	−242	11 100	−122	320
623	−122	8 760	−179	11 900	−93	1 380
673	−95	6 480	−137	9 740	−72	1 470
723	−75	4 830	−108	7 520	−57	1 315
773	−60	3 670	−87	5 780	−45	1 120

are all smaller than those of real water, although this model possesses an elevated value (2.14 D) of its gas-phase dipole moment.

The short-range interaction of the PPC model was taken to be a LJ potential centred on the oxygen. The LJ parameters, ϵ_{LJ}=0.6 kJ/mol and σ=3.234 Å, were optimized to give the correct energy, self-diffusion coefficient, and structure for water at 25 °C.[22] We remark that unlike other polarizable models, which typically execute at least three times more slowly than effective potential models, a comparable calculation with the PPC model runs only 1.5 times more slowly than a simulation with SPC/E water.

APPENDIX C: SECOND AND THIRD VIRIAL COEFFICIENT DATA

Detailed numerical data for the second and third virial coefficients can be found in Table IV for the three models considered in this study. A copy of the FORTRAN code used to calculate the third virial coefficients for TIP4P water can be obtained by sending a request via electron mail to ''kusalik@ac.dal.ca.''

[1] E. A. Mason and T. H. Spurling, *The Virial Equation of State* (Pergamon, New York, 1969).
[2] J. O. Hirschfelder, C. F. Curtiss, and R. B. Bird, *Molecular Theory of Gases and Liquids* (Wiley, New York, 1964).
[3] D. A. McQuarrie, *Statistical Thermodynamics* (Harper & Row, New York, 1973).
[4] J. A. Barker and A. Pompe, Aust. J. Chem. **21**, 1683 (1968).
[5] C. H. J. Johnson and T. H. Spurling, Aust. J. Chem. **24**, 1567 (1971).
[6] C. H. J. Johnson, A. Pompe, and T. H. Spurling, Aust. J. Chem. **25**, 2021 (1972).
[7] D. J. Evans and R. O. Watts, Mol. Phys. **28**, 1233 (1974).
[8] R. E. Kozack and P. C. Jordan, J. Chem. Phys. **96**, 3120 (1992).
[9] P. Cieplak, P. Kollman, and T. Lybrand, J. Chem. Phys. **92**, 6755 (1990).
[10] J. R. Reimers, R. O. Watts, and M. L. Klein, Chem. Phys. **64**, 95 (1982).
[11] C. Joslin and S. Goldman, Mol. Phys. **79**, 499 (1993).
[12] H. Conroy, J. Chem. Phys. **47**, 5307 (1967).
[13] NAG Ltd., Wilkinson House, Jordan Hill Road, Oxford OX2 8DR, U.K.
[14] N. M. Korobov, Dokl. Acad. Nauk. SSSR **115**, 1062 (1957); *Number Theoretic Methods in Approximate Analysis* (Fizmatgiz, Berlin, 1963).
[15] B. Lautrup, Proc. Second Colloquium on Advanced Methods in Theoretical Physics, Marseilles, 1971.
[16] T. W. Sag and G. Szekeres, Math. Comput. **18**, 245 (1964).
[17] P. Van Dooren and L. De Ridder, J. Comput. Appl. Math. **2**, 207 (1976); A. C. Genz and A. A. Malik, *ibid*. **6**, 295 (1980).
[18] Using product methods, 30 million points would afford only about 4 points in each of the 12 dimensions of the numerical integral.
[19] H. J. C. Berendsen, J. R. Grigera, and T. P. Straatsma, J. Phys. Chem. **91**, 6269 (1987).
[20] W. L. Jorgensen, J. Chandrasekhar, J. D. Madura, R. W. Impey, and M. L. Klein, J. Chem. Phys. **79**, 926 (1983).
[21] P. G. Kusalik and I. M. Svishchev (unpublished).
[22] P. G. Kusalik and I. M. Svishchev, Science **265**, 1219 (1994).
[23] P. G. Hill and R. D. C. MacMillan, Ind. Eng. Chem. Res. **27**, 874 (1988).
[24] G. S. Kell, G. E. McLaurin, and E. Whalley, Proc. R. Soc. London Ser. A **425**, 49 (1989).
[25] M. P. Vulalovich, M. S. Trakhtengerts, and G. A. Spiridonov, Teploenergetika **14**, 65 (1967); Heat Pwr. Eng., Wash. **14**, 86 (1967).
[26] R. W. Crain, Jr. and R. E. Sonntag, Adv. Cryogen. Engng. **11**, 379 (1966).
[27] A. E. Hoover, F. B. Canfield, R. Kobayashi, and T. W. Leland, Jr., J. Chem. Engng. Data **9**, 568 (1964).
[28] A. E. Hoover, I. Nagata, T. W. Leland, Jr., and R. Kobayashi, J. Chem. Phys. **48**, 2633 (1968).
[29] Y. Guissani and B. Guillot, J. Chem. Phys. **98**, 8221 (1993).